

Strangeness-driven phase transition in (proto)-neutron star matter

F. Gulminelli¹, Ad. R. Raduta², M. Oertel³, and J. Margueron⁴

¹ *CNRS and ENSICAEN, UMR6534, LPC, 14050 Caen cédex, France*

² *IFIN-HH, Bucharest-Magurele, POB-MG6, Romania*

³ *LUTH, CNRS, Observatoire de Paris, Université Paris Diderot, 5 place Jules Janssen, 92195 Meudon, France*

⁴ *Institut de Physique Nucléaire, IN2P3-CNRS, Université Paris-Sud, F-91406 Orsay cedex, France.*

The phase diagram of a system constituted of neutrons, protons, Λ -hyperons and electrons is evaluated in the mean-field approximation in the complete three-dimensional space given by the baryon, lepton and strange charge. It is shown that the phase diagram at sub-saturation densities is strongly affected by the electromagnetic interaction, while it is almost independent of the electric charge at supra-saturation density. As a consequence, stellar matter under the condition of strangeness equilibrium is expected to experience a first as well as a second-order strangeness-driven phase transition at high density, while the liquid-gas phase transition is expected to be quenched. An RPA calculation indicates that the presence of this critical point might have sizable implications for the neutrino propagation in core-collapse supernovae.

PACS numbers: 26.50.+x, 26.60.-c 21.65.Mn, 64.10.+h, 64.60.Bd,

I. INTRODUCTION

Supernova explosions following the gravitational collapse of a massive star ($M \gtrsim 8M_\odot$) are among the most fascinating events in the universe as they radiate as much energy as the sun is expected to emit over its whole life span [1]. Nuclear physics is an essential ingredient in the numerical simulations which aim to describe these events, since realistic astrophysical descriptions of the collapse and post-bounce evolution rely on the accuracy of the implementation of weak processes and equation(s) of state (EOS) [2, 3]. Determining the EOS constitutes a particularly difficult task since phenomenology ranges from a quasi-ideal un-homogeneous gas to strongly interacting uniform matter and, potentially, deconfined quark-matter. The situation is even more difficult if phase transitions are experienced, since mean-field models fail in such situations [4].

The Coulomb-quenched liquid-gas (LG) phase transition taking place at densities smaller than the nuclear saturation density ($n_0 = 0.16 \text{ fm}^{-3}$) is, probably, the most notorious and best understood case [5–9]. At highest densities, a quark-gluon plasma is expected, but predictions on the exact location of the transition are strongly model dependent [10]. In the intermediate density domain simple energetic considerations show that additional degrees of freedom may be available, such as hyperons, nuclear resonances, mesons or muons [11]. The possibility that the onset of hyperons could pass via a first order phase transition in neutron stars has been evoked in Ref. [12], using a relativistic mean field model (RMF), and in Ref. [13], a phase transition between phases with different hyperonic species has been observed for cold matter. The possibility of a first order phase transition to hyperonic matter in effective RMF models has been discussed in Refs. [14–16], too. Within the latter models, the phase transition region is located at sub-saturation densities,

and is thus not relevant for star matter. Using a simple two-component (n, Λ) model, we have recently studied the complete phase diagram of strange baryonic matter showing that it exhibits a complex structure with first and second order phase transitions [17]. However, the exploratory calculation of Ref. [17] neglects the fact that in addition to baryon number B and strangeness S , the charge Q and lepton L quantum numbers are also populated. The thermodynamics of the complete system should thus be studied in the four-dimensional space of the associated charges n_B, n_S, n_L, n_Q . The strict electroneutrality constraint $n_Q = 0$, necessary to obtain a thermodynamic limit [18], makes the physical space three-dimensional. As it is known from the EOS studies at sub-saturation density [19], the introduction of the charge degree of freedom can have a very strong influence on the phase diagram and cannot be neglected. In this work we therefore introduce a four-component model constituted of neutrons, protons, electrons and Λ -hyperons. Electrons are treated as an ideal gas.

We present, in sec. II of this paper, the thermodynamics and phase transition of the n, p, e and Λ system, and discuss the influence of the Coulomb interaction. The consequence of the phase transition on the cooling of proto-neutron stars, through the neutrino mean free path, is qualitatively discussed in sec. III. Finally, we present our conclusions in sec. IV.

II. THERMODYNAMICS OF A N, P, Λ SYSTEM WITH ELECTRONS

In the widely used mean-field approximation [11, 20–26] the total baryonic energy density is given by the sum of the mass, kinetic and potential energy density functionals which represents a surface in the three-dimensional space defined by the baryon, strange and

charge density given, in our case, by $n_B = n_n + n_p + n_\Lambda$, $n_S = -n_\Lambda$ and $n_Q = n_p$. In the non-relativistic formalism valid in the considered domains of density and temperature it reads

$$e_B = \sum_{i=n,p,\Lambda} \left(n_i m_i c^2 + \frac{\hbar^2}{2m_i} \tau_i \right) + e_{pot}(n_n, n_p, n_\Lambda) \quad (1)$$

The single-particle densities are given by the Fermi integrals

$$n_i = \frac{4\pi}{h^3} \left(\frac{2m_i}{\beta} \right)^{\frac{3}{2}} F_{\frac{1}{2}}(\beta \tilde{\mu}_i); \quad \tau_i = \frac{8\pi^3}{h^5} \left(\frac{2m_i}{\beta} \right)^{\frac{5}{2}} F_{\frac{3}{2}}(\beta \tilde{\mu}_i), \quad (2)$$

where $F_\nu(\eta) = \int_0^\infty dx \frac{x^\nu}{1+\exp(x-\eta)}$ is the Fermi-Dirac integral, $\beta = T^{-1}$ is the inverse temperature, m_i is the effective i -particle mass and $\tilde{\mu}_i$ is the effective chemical potential of the i -species self-defined by the single-particle density.

A. The model

A full thermodynamics characterization of the system is provided by the pressure $P_B = T s_B - e_B + \sum_i \mu_i n_i$ together with the entropy density s_B in mean-field,

$$s_B = \sum_{i,p,\Lambda} \left[\frac{10\hbar^2}{6m_i} \beta \tau_i - n_i \beta \tilde{\mu}_i \right]. \quad (3)$$

The thermodynamical definition $n_i \doteq \left(\frac{\partial P}{\partial \mu_i} \right) |_\beta$ allows to infer the relation among the chemical potentials μ_i and the effective parameters $\tilde{\mu}_i$ as $\mu_i = \tilde{\mu}_i + m_i c^2 + U_i$, with $U_i = \partial e_{pot} / \partial n_i$.

Within the numerical applications we shall use the potential energy density proposed by Balberg and Gal [27],

$$e_{pot}(n_n, n_p, n_\Lambda) = \sum_{i,j=\{n,p,\Lambda\}} (a_{ij} n_i n_j + b_{ij} t_i t_j n_i n_j) + c_{ij} \frac{1}{n_i + n_j} (n_i^{\gamma_{ij}+1} n_j + n_j^{\gamma_{ij}+1} n_i), \quad (4)$$

accounting for nucleon-nucleon, nucleon- Λ and Λ - Λ interactions. t_i denotes the third isospin component of particle i . In the non-strange sector the form of the interaction is the same as in the widely used Lattimer-Swesty [28] EOS.

Let us mention that the observation of a neutron star (PSR J 1614-2230) with a mass of almost two solar masses [29] imposes stringent constraints on the hyperonic interaction in dense neutron star matter. The maximum mass for a $n, p, \Lambda + e$ system as studied in the present manuscript is $2.04 M_\odot$ with the parameter set BG I for the coupling constants (see Table I) in agreement with the mass of PSR J 1614-2230. Including all hyperonic degrees of freedom, the maximum neutron star

mass obtained with parametrisation BG I decreases and becomes slightly too low. However, the qualitative results discussed here about the thermodynamics of the system and the consequences on the neutrino mean free path are independent of the parametrisation used. In particular, the same qualitative results are obtained with the parametrisations from Ref. [21], in agreement with the mass of PSR J 1614-2230 even upon including all the different hyperons. Quantitative differences are very small, such that we have chosen here to use for numerical applications one parametrisation from the original paper by Balberg and Gal [27], BG I.

B. Instabilities and phase-transition

Matter stability with respect to phase separation can be checked in any point of the extensive variable space by analyzing the eigen-values of the curvature matrix [5, 30, 31], $C_{ij} = \partial^2 f(\{n_l\}_{l=\{i,j,k\}}) / \partial n_i \partial n_j$, where $i, j, k = B, S, Q$ and $f = e_{tot} - T s_{tot}$ is the total free-energy. The occurrence of, at least, one negative eigen-value in a certain domain of (n_B, n_S, n_Q) means that the system is unstable versus phase separation. The associated 3-dimensional Gibbs construction can be reduced to a simpler 1-dimensional Maxwell construction [5] by performing a Legendre transformation with respect to two out of the three chemical potentials $\mu_B = \mu_n$, $\mu_S = -\mu_\Lambda + \mu_n$ and $\mu_Q = \mu_p - \mu_n$. We have chosen to work in the hybrid ensemble (n_B, μ_S, μ_Q) defined by:

$$\bar{f}_{baryon}(n_B, \mu_S, \mu_Q) = f_{baryon} - \mu_S n_S - \mu_Q n_Q, \quad (5)$$

If the associated equation of state $\mu_B = \partial \bar{f}_{baryon}(n_B, \mu_S, \mu_Q) / \partial n_B$ as a function of n_B presents a slope inversion, the relation $\mu_B(n_B)$ is three-valued within a given interval of μ_B . Then a Maxwell equal-area construction on this function allows defining two values $n_B^{(1)}, n_B^{(2)}$, which are characterized by the complete Gibbs equilibrium conditions $(P, \mu_B, \mu_S, \mu_Q)_{(1)} = (P, \mu_B, \mu_S, \mu_Q)_{(2)}$ for a multi-component system. The hyper-surface connecting the two points $(n_B, n_S, n_Q)_{(1)}, (n_B, n_S, n_Q)_{(2)}$ is the usual Gibbs construction. This procedure is independent of the choice of the densities (here: n_S, n_Q) to be Legendre-transformed, provided the order parameter has a non-vanishing component along the remaining density (here: n_B). If this was not the case, that is if there was no jump in n_B at the phase transition, $n_B^{(1)} = n_B^{(2)}$, the information on the phase transition could not be extracted from the hybrid ensemble eq.(5). We have verified that this is never the case, and the phase transition we will identify always separates a more diluted (lower n_B) from a denser (higher n_B) phase. For a generic physical multi-component system, this is not always the case and in the general case the convexity properties of the free energy have to be examined with care in order to identify phase transitions in such systems. In particular for our specific physics application

TABLE I: Coupling constants corresponding to the stiffest interaction proposed in Ref. [27].

Parameter set	a_{NN} MeV fm ³	b_{NN} MeV fm ³	c_{NN} MeV fm ^{3δ}	$a_{\Lambda\Lambda}$ MeV fm ³	$c_{\Lambda\Lambda}$ MeV fm ^{3γ_{NN}}	$a_{\Lambda N}$ MeV fm ³	$c_{\Lambda N}$ MeV fm ^{3γ_{ΛN}}	γ_{NN}	$\gamma_{\Lambda N}$
BGI	-784.4	214.2	1936.	-486.2	1553.6	-340.	1087.5	2	2

of strangeness phase transition, we will explicitly show that the charge density is almost unaffected by the phase transition. This means that the concavity of the free energy $\bar{f}_{baryon}(\mu_B, \mu_S, n_Q)$ as a function of n_Q is extremely small. This means that working in that statistical ensemble would have rendered the observation of the phase transition very difficult. We stress that the one-dimensional Maxwell construction in the hybrid ensemble eq. (5), as long as a n_B jump occurs through the phase transition as it does here, is strictly equivalent to the complete Gibbs construction. In particular, the pressure, as function of one density with the other densities kept constant, has not a constant value in the mixed phase [5]. For instance, $P(n_B)$ at fixed n_S, n_Q is not constant in the mixed phase region. On the contrary, a Maxwell construction on $P(n_B)$ or $\mu_B(n_B)$ at constant values of n_S, n_Q is never theoretically justified.

The upper part of Fig. 1 illustrates the projection of the $T = 0$ phase diagram in the $n_B - n_S$ plane for $\mu_S = 0$. The arrows mark the direction of phase separation which, in case of phase coexistence, coincides with the order parameter. Two phase-coexistence domains may be identified. The one lying along $n_S = 0$ at sub-saturation density corresponds to the well known LG like phase transition taking place in dilute nuclear matter [5]. The second domain lies at supra-saturation densities ($n_B \gtrsim 2n_0$), and the direction of phase separation is dominated by the strange density. In the density range shown by the figure, this domain is not upper limited in ρ_B . We observe a bending at very high density meaning that the domain is finite as for the sub-saturation LG transition, but since we do not consider these densities as being realistically described within the present model, we refrain from showing the whole domain here. This transition is consistent with our previous findings within a simpler 2D model [17], though it obviously depends on the assumed strengths of the NN, NY and YY -interactions. It is at first sight surprising to observe that the coexistence border of the latter transition is given by simple straight lines. In principle the coexistence borders of a first order phase transition with three conserved charges are given by two surfaces in the three dimensional space. For their projection on the $n_B - n_S$ plane to be given by a one-dimensional curve, these surfaces have to be perpendicular to that plane, that is independent of n_Q . The observed independence on the electric charge shows that the strange charge is the dominant order parameter for this transition. However, we can expect that some dependence on the electric charge would arise if charged strange particles were included, because of the correlation which

would then exist between n_Q and n_S . The middle part of Fig. 1 illustrates the projection of the phase coexistence domains in the $n_B - n_Q$ plane for $\mu_S = 0$, corresponding to the strangeness-equilibrium condition which is relevant for star matter. As discussed above, the coexistence domain being three-dimensional this representation depends on the value of the third variable given by μ_S (or n_S). The well-known isospin dependence of the LG phase transition occurring at $n_S = 0$ [5] is apparent. We have just noticed that the order parameter of the strangeness phase transition is given by a combination of the strange and baryonic density. Not surprisingly, the direction of phase separation of this transition in the $n_B - n_Q$ plane is thus dominated by the baryonic density. The order parameter component in the direction of the electric charge can be understood as due to the correlation between the different densities. We are facing a transition between a relatively diluted, non-strange phase to a relatively dense, more strange one. Since Λ 's are neutral, the positively charged component of the baryonic density is relatively less important in the dense phase, which explains the slope of the separation direction.

Fig. 2 offers the complementary image on how the two phase coexistence domains look like when plotted with respect to $\mu_S - \mu_B$. In this case the condition $\mu_S = 0$ is released and alternative arbitrary constraints on $\mu_Q = -50, 0, 50$ MeV are imposed. The absence of Λ -hyperons at sub-saturation densities makes the conjugated chemical potential undefined. Mathematically, this means that any $\mu_\Lambda \leq (U_\Lambda + m_\Lambda c^2)$ is possible. This makes μ_S span a semi-infinite domain lower limited by $(\mu_n - U_\Lambda - m_\Lambda c^2)$. Reminding that - in $\mu_n - \mu_p$ coordinates - the nuclear matter LG phase coexistence is figured by a curve whose extremities are the critical points, it is easy to understand that, by fixing μ_Q , one fixes both μ_n and μ_p . Now, one can straightforwardly identify the semi-infinite horizontal coexisting lines as the ones corresponding to LG. The strangeness-driven phase coexistence at fixed μ_Q appears in $\mu_S - \mu_B$ as two merged semi-infinite linear segments. The merging point corresponds to the state where the equilibrium counter-part of the dense phase jumps from vacuum (low μ_S) to a dilute mixture (high μ_S).

C. Influence of the Coulomb interaction

We now turn to investigate the influence of Coulomb effects on the phase diagram. For simplicity, we will con-

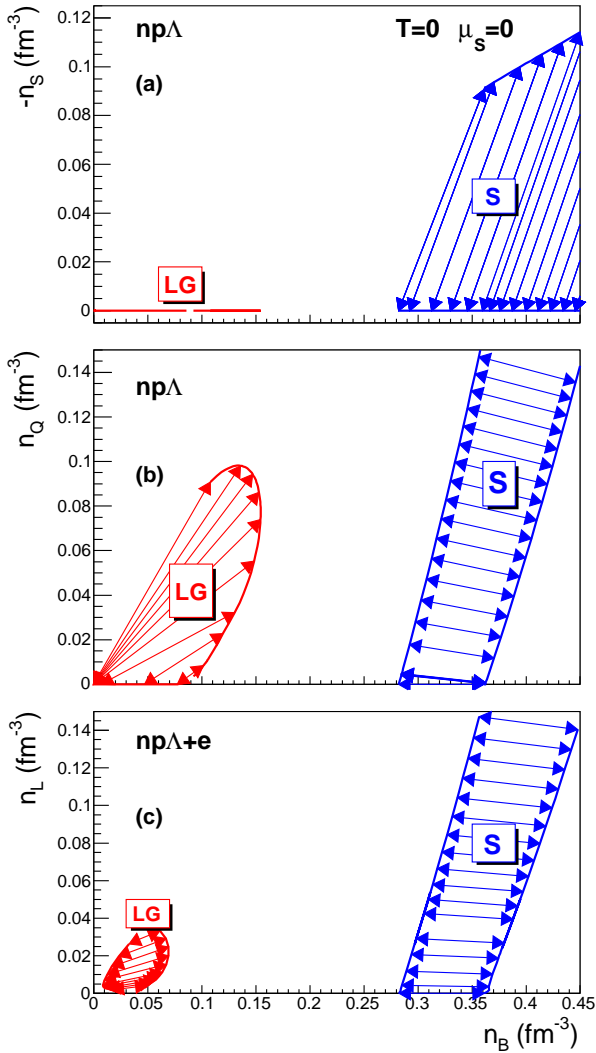


FIG. 1: (Color online) Borders of the phase-coexistence domains at $T=0$ and $\mu_S=0$. Upper (middle): (n, p, Λ) -mixture in $n_B - n_S$ ($n_B - n_C$) coordinates. Lower: (n, p, Λ, e) -mixture in $n_B - n_L$ coordinates. Red: liquid-gas phase transition of non-strange dilute nuclear matter; blue: non-strange to strange phase transition. The arrows mark the directions of phase separation.

sider only electrons and neglect other charged leptons or mesons.

Electrons are coupled to charged baryons through the electromagnetic interaction, which can modify the baryonic phase diagram. However, the charge neutrality condition $n_Q = 0$ makes the associated chemical potential μ_Q ill-defined and keeps the problem three-dimensional [18]. Since in homogeneous matter with the condition $n_Q = 0$ the Coulomb interaction exactly vanishes [18], the total mean field pressure can be written as a sum over independent terms $P_B + P_L + P_\gamma + P_\nu + \dots$. We shall still concentrate on the P_B contribution, as the

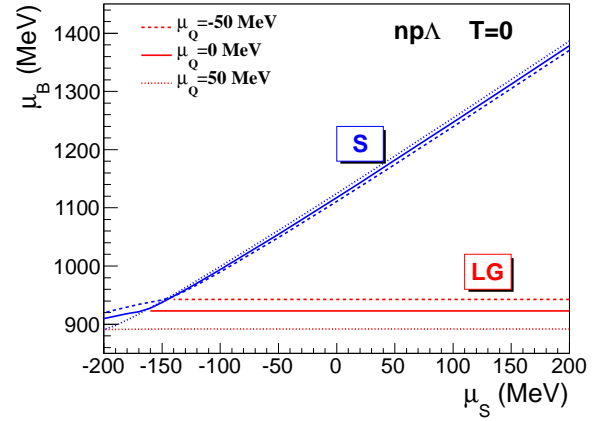


FIG. 2: (Color online) Borders of the phase-coexistence domains corresponding to the (n, p, Λ) -mixture at $T=0$ and $\mu_Q = -50, 0, 50$ MeV in $\mu_B - \mu_S$ coordinates. Red: liquid-gas phase transition of non-strange dilute nuclear matter; blue: phase transition from non-strange to strange compressed baryonic matter.

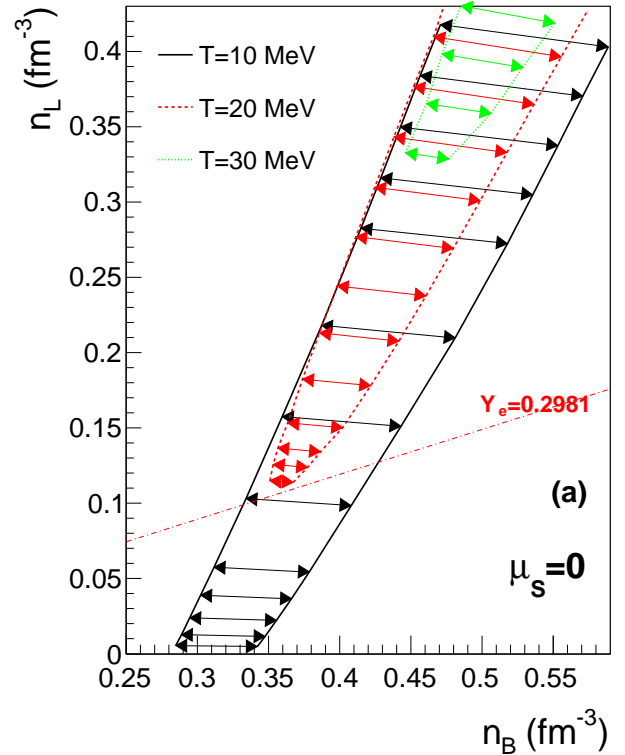


FIG. 3: (Color online) Borders of the strangeness driven phase transition domain corresponding to the neutral net-charge (n, p, Λ, e) -mixture at $T=10, 20, 30$ MeV and $\mu_S=0$ in $n_B - n_L$ coordinates. The dot-dashed line marks, for $T=20$ MeV, a path of constant $Y_e = 0.2981$.

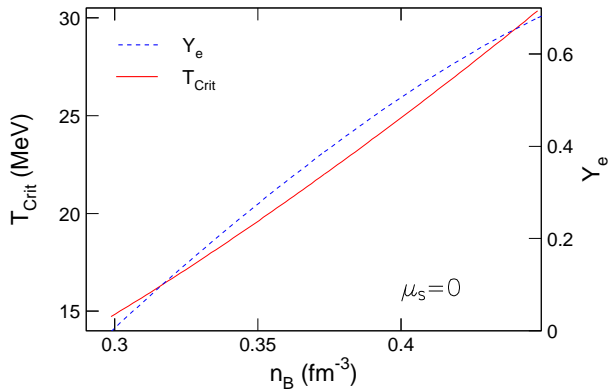


FIG. 4: (Color online) Electron fraction, Y_e , and n_B at the corresponding critical temperature for $\mu_S = 0$.

other terms do not affect the convexity properties of the thermodynamical potential on which phase transitions rely. We have constructed the full phase diagram of the $(np\Lambda e)$ system in the (n_B, n_S, n_L) space using the hybrid ensemble

$$\bar{f}_{baryon}(n_B, \mu_S, \mu_L) = f_{baryon} - \mu_S n_S - \mu_L n_L. \quad (6)$$

In practice, the charge neutrality condition gives $n_p = n_e$, which allows to infer the electron chemical potential, μ_e , via

$$n_e = \frac{1}{3\pi^2} \left(\frac{\mu_e}{\hbar c} \right)^3 \left[1 + \mu_e^{-2} \left(\pi^2 T^2 - \frac{1}{2} m_e^2 c^4 \right) \right], \quad (7)$$

and to obtain $\mu_L = \mu_p - \mu_n + \mu_e$. Note that $n_e = n_{e^-} - n_{e^+} = n_L (= n_p)$ stands here for the net electron density. If neutrinos were in equilibrium, then μ_L would correspond to the electron neutrino chemical potential. In particular, in a cold neutron star in β -equilibrium we would have $\mu_L = 0$ fixing n_e . In core collapse events, on the other hand, neutrinos cannot be considered in equilibrium in the major part of the system. Here we want to study the entire phase diagram, not restricting to β -equilibrium, and we therefore leave μ_L free. Neutrinos, even in equilibrium, would not change the phase properties, and are thus neglected for the sake of simplicity in the present discussion.

The lowest panel of Fig. 1 depicts the phase coexistence regions of the $(np\Lambda e)$ system at $T = 0$ and $\mu_S = 0$. In agreement with the results of Ref. [19, 32], a strong Coulomb quenching of the LG-phase transition is obtained. However, the coexistence domain of the strangeness-driven phase transition is practically unmodified. This can be easily understood from the fact that the effect of the neutrality condition $n_Q = 0$ on the two phase transitions is very different. The phase transition at sub-saturation density has the total baryonic density as order parameter. At such densities, n_B is strongly correlated to n_p because of the nuclear sym-

metry energy which favors symmetric $n_n = n_p$ matter. The phase transition thus implies a discontinuity in $n_p = n_e$, which is strongly disfavored by the huge electron incompressibility [19]. At supersaturation densities the order parameter is given by n_S which is very loosely correlated to n_Q . The phase transition thus does not imply any strong change in the electron distribution and the presence of electrons thus does not influence much the phase diagram.

The temperature dependence of the phase diagram along $\mu_S = 0$ is presented in Fig. 3. We can observe that the direction of phase separation is almost independent of T . More interesting, starting from a finite value of T , a critical point appears and survives up to very high temperature. On Fig. 4 the critical temperature and the electron fraction $Y_e = n_e/n_B$ are shown as a function of baryon density. These values are typically reached within the cooling proto-neutron star, meaning that effects of criticality should be experienced.

III. EFFECT OF THE PHASE-TRANSITION ON THE NEUTRINO MEAN FREE PATH

The cooling of proto-neutron stars is mostly driven by neutrino diffusion during the first seconds. To explore the consequence of criticality for the cooling of proto-neutron star, we therefore turn to calculate the mean free path for the neutrino scattering off n, p, and Λ particles including the long-range correlations, essential for the study of criticality, in the linear response approximation. In the non-relativistic limit for the baryonic components, the mean free path at temperature T of a neutrino with initial energy E_ν is given by $1/\lambda = 1/\lambda^V + 1/\lambda^A$ [33, 34] where the contribution of the vector channel is defined as,

$$\frac{1}{\lambda^V(E_\nu, T)} = \frac{G_F^2}{16\pi^2} \int (1 + \cos\theta) \mathcal{S}^V(q, T) (1 - f_\nu(\mathbf{k}_3)) d\mathbf{k}_3, \quad (8)$$

and that of the axial channel,

$$\frac{1}{\lambda^A(E_\nu, T)} = \frac{G_F^2}{16\pi^2} \int (3 - \cos\theta) \mathcal{S}^A(q, T) (1 - f_\nu(\mathbf{k}_3)) d\mathbf{k}_3. \quad (9)$$

In Eqs. (8)-(9), G_F is the Fermi constant, θ is the angle between the initial and final neutrino momentum ($=\mathbf{k}_3$), q is the transferred energy-momentum, $q = (\omega, \mathbf{q})$, and f_ν is the Fermi-Dirac distribution of the outgoing neutrino. \mathcal{S}^V (\mathcal{S}^A) are the dynamical response function in the vector (axial) channel. Since this study is focused on the impact of the density fluctuations close to the critical point, only the vector channel is considered. For densities close to the critical point, spin-density fluctuations are however expected to be small [35, 36].

The dynamical response function in the vector channel

is defined as

$$S^V(q, T) = -\frac{2}{\pi} \frac{1}{1 - \exp(-\omega/T)} \times \begin{pmatrix} c_V^n & c_V^p & c_V^\Lambda \end{pmatrix} \Pi^V(q, T) \begin{pmatrix} c_V^n \\ c_V^p \\ c_V^\Lambda \end{pmatrix}, \quad (10)$$

where $\Pi^V(q, T)$ is the vector-polarization matrix for the three species n, p, and Λ , given by the Lindhard functions in the case of the mean-field approximation and by the solution of the Bethe-Salpeter equations in the case of the mean-field+RPA approximation [33, 34, 36]. The vector coupling constants are set to be: -1 (n), 0.08 (p), -1 (Λ) [37]. The residual p-h interaction is derived from the potential energy (5) and is closely related to the curvature matrix without electrons [31].

The neutrino mean free path along an arbitrary $Y_e = 0.2981$ trajectory in the phase diagram which passes by the critical point (see dot-dashed line in Fig. 3(a)) is shown in Fig. 5. As expected, the RPA correlations strongly reduce the neutrino mean free path close to the critical point, similar to the critical opalescence effect observed for the photon scattering off matter in critical water. The ratio of the neutrino mean free path in mean-field+RPA approximation over that at the mean-field level is shown in panel (b) exploring different neutrino energies around the neutrino chemical potential defined at beta equilibrium. The effect of the RPA correlations around the critical point is almost independent of the neutrino energy in agreement with the interpretation as critical opalescence.

IV. CONCLUSIONS

To conclude, we have studied the phase diagram of a mixture constituted of interacting neutrons, protons

and Λ -hyperons under the condition of strangeness-equilibrium, relevant for supernovae and neutron star physics. At supra-saturation densities, a strangeness-driven phase transition can take place, depending on the assumed strengths of nucleon- Λ and Λ - Λ interactions [17]. This second transition survives the screening effect of electrons and persists over a large domain of temperatures such that it may have an impact on star phenomenology. For a first study of this equation of state (EoS) within core-collapse supernovae, see [38]. In addition to the EoS, linear response theory shows that the neutrino mean-free path dramatically decreases close to the critical point of this phase transition, which occurs in a thermodynamic domain accessible to newly-born proto-neutron stars.

These results present a first step, and quantitative results might be somewhat modified in the presence of other strange- and non-strange baryonic, leptonic or mesonic degrees of freedom. This work is in progress and it will make the subject of a forthcoming publication.

Acknowledgments

This work has been partially funded by the SN2NS project ANR-10-BLAN-0503 and it has been supported by Compstar, a research networking program of the European Science foundation. Ad. R. R acknowledges partial support from the Romanian National Authority for Scientific Research under grants PN-II-ID-PCE-2011-3-0092 and PN 09 37 01 05 and kind hospitality from LPC-Caen.

-
- [1] H. A. Bethe, Supernova mechanisms. *Reviews of Modern Physics*, **62**, 801 (1990).
 - [2] H.-T. Janka, K. Langanke, A. Marek, G. Martinez-Pinedo and B. Müller, *Phys. Rept.* **442** (2007) 38.
 - [3] J. M. Lattimer and M. Prakash, *Phys. Rept.* **442**, 109 (2007).
 - [4] N. K. Glendenning, *Phys. Rep.* **342**, 394 (2001).
 - [5] C. Ducoin, Ph. Chomaz and F. Gulminelli, *Nucl. Phys. A* **771**, 68 (2006).
 - [6] M. Barranco and J. R. Buchler, *Phys. Rev. C* **24**, 1191 (1981).
 - [7] S. Shlomo and V. M. Kolomietz, *Rep. Prog. Phys.* **68**, 1 (2005).
 - [8] F. Douchin, P. Haensel and J. Meyer, *Nucl. Phys. A* **665**, 419 (2000).
 - [9] A. Rios, *Nucl. Phys. A* **845**, 58 (2010).
 - [10] I. Sagert *et al.*, *Phys. Rev. Lett.* **102**, 081101 (2009).
 - [11] N. Glendenning, *Phys. Lett.* **B114**, 392 (1982).
 - [12] J. Schaffner-Bielich, M. Hanauske, H. Stöcker and W. Greiner, *Phys. Rev. Lett.* **89** (2002) 171101.
 - [13] J. Schaffner-Bielich and A. Gal, *Phys. Rev. C* **62** (2000) 034311.
 - [14] P. Wang, D. B. Leinweber, A. W. Thomas, A. G. Williams and , *Phys. Rev. C* **70** (2004) 055204.
 - [15] L. Yang, W. L. Qian, R. -K. Su, H. Q. Song and , *Phys. Rev. C* **70** (2004) 045207.
 - [16] L. Yang, S. Y. Yin, W. L. Qian, R. -k. Su and , *Phys. Rev. C* **73** (2006) 025203.
 - [17] F. Gulminelli, Ad. R. Raduta and M. Oertel, *Phys. Rev. C* **86**, 025805 (2012).
 - [18] C. Ducoin, K. H. O. Hasnaoui, P. Napolitani, Ph. Chomaz and F. Gulminelli, *Phys. Rev. C* **75** 065805 (2007).
 - [19] C. Ducoin, Ph. Chomaz and F. Gulminelli, *Nucl. Phys.*

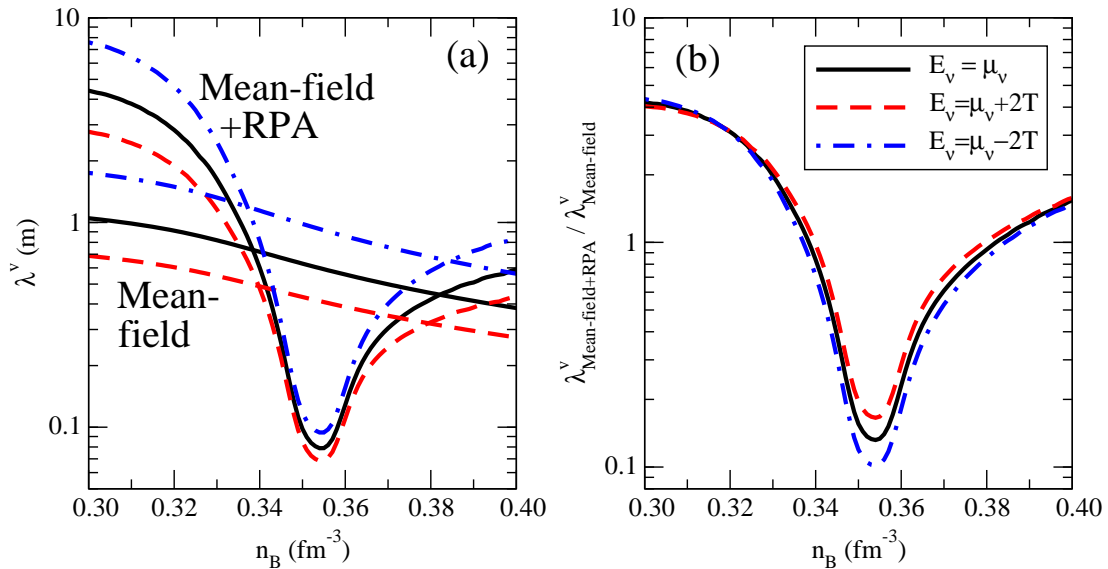


FIG. 5: (Color online) (a) Neutrino mean free path for the scattering off n, p, and Λ at $T = 20$ MeV along a constant- $Y_e = 0.2981$ trajectory in the phase diagram for $E_\nu = \mu_\nu$, $\mu_\nu \pm T$ as a function of the baryonic density ρ . The result of the mean-field approximation is compared to the mean-field+RPA. (b) The ratio of the mean free path within mean-field+RPA over mean-field approximation is shown.

- A789**, 403 (2007).
- [20] J. R. Stone, P. A. M. Guichon, and A. W. Thomas, ArXiv e-prints (2010), 1012.2919.
- [21] M. Oertel, A. F. Fantina and J. Novak, Phys. Rev. C **85**, 055806 (2012).
- [22] S. Weissenborn, D. Chatterjee and J. Schaffner-Bielich, Nucl. Phys. **A881**, 62 (2012).
- [23] I. Bednarek, P. Haensel, J. L. Zdunik, M. Bejger and R. Manka, Astron. & Astrophys. **543** (2012) 157.
- [24] F. Hofmann, C. Keil and H. Lenske, Phys. Rev. C **64**, 025804 (2001).
- [25] L. Bonanno and A. Sedrakian, Astron. & Astrophys. **539**, A16 (2012).
- [26] R. Lastowiecki, D. Blaschke, H. Grigorian and S. Typel, Acta Phys. Pol. B Proc. Suppl. **5**, 535 (2012).
- [27] S. Balberg and A. Gal, Nucl. Phys. **A625**, 435 (1997).
- [28] J. M. Lattimer and F. D. Swesty, Nucl. Phys. **A535**, 331 (1991).
- [29] P. Demorest *et al.*, Nature **467** (2010) 1081.
- [30] J. Margueron and Ph. Chomaz, Phys. Rev. C **67**, 041602 (2003).
- [31] C. Ducoin, J. Margueron and Ph. Chomaz, Nucl. Phys. **A 809**, 30 (2008).
- [32] C. Providencia, L. Brito, S. S. Avancini, D. P. Menezes and Ph. Chomaz, Phys. Rev. C **73**, 025805 (2006).
- [33] N. Iwamoto and C.J. Pethick, Phys. Rev. **D 25**, 313 (1982).
- [34] J. Navarro, E.S. Hernandez and D. Vautherin, Phys. Rev. **C 60**, 045801 (1999).
- [35] A. Polls, A. Ramos and I. Vidaña, Phys. Rev. C **65**, 035804 (2002).
- [36] J. Margueron, I. Vidaña and I. Bombaci, Phys. Rev. C **68**, 055806 (2003).
- [37] S. Reddy, M. Prakash and J.M. Lattimer, Phys. Rev. **D 58**, 013009 (1998).
- [38] B. Peres, M. Oertel and J. Novak, Phys. Rev. **D 87**, 043006 (2013).